



HAL
open science

Production of al foams using the SDP method: Processing parameters and introduction of a new sintering device

J.H. Cadena, Ignacio A. Figueroa, M.A. Suarez, O. Novelo-Peralta, G. González, G. A. Lara-Rodríguez, Ismeli Alfonso

► **To cite this version:**

J.H. Cadena, Ignacio A. Figueroa, M.A. Suarez, O. Novelo-Peralta, G. González, et al.. Production of al foams using the SDP method: Processing parameters and introduction of a new sintering device. Journal of Mining and Metallurgy, Section B: Metallurgy, 2016, 521 (1), pp.47-52. <10.2298/JMMB150128024C>. <hal-02197688>

HAL Id: hal-02197688

<https://hal.science/hal-02197688v1>

Submitted on 30 Jul 2019

HAL is a multi-disciplinary open access archive for the deposit and dissemination of scientific research documents, whether they are published or not. The documents may come from teaching and research institutions in France or abroad, or from public or private research centers.

L'archive ouverte pluridisciplinaire **HAL**, est destinée au dépôt et à la diffusion de documents scientifiques de niveau recherche, publiés ou non, émanant des établissements d'enseignement et de recherche français ou étrangers, des laboratoires publics ou privés.



HAL Authorization

PRODUCTION OF Al FOAMS USING THE SDP METHOD: PROCESSING PARAMETERS AND INTRODUCTION OF A NEW SINTERING DEVICE

J. H. Cadena^a, I. A. Figueroa^{a*}, M. A. Suarez^a, O. Novelo-Peralta^a, G. González^{a,b},
G.A. Lara-Rodríguez^a, I. Alfonso^a

^a Universidad Nacional Autónoma de México, Instituto de Investigaciones en Materiales, México

^b Laboratoire Procédés et Ingénierie Mécanique et Matériaux ENSAM, Paris, France

Abstract

The processing of aluminum (Al) foams with maximum porosity of around 70 %, regular pore size and interconnected pores were successfully produced by means of the powder metallurgy method of Sintering Dissolution Process (SDP). The metal powder used for the present study was Al powder with 99.5 % of purity and diameters between 75 μm and 200 μm. The chosen Space Holder Particles (SHP) were spherical carbamide CH₄N₂O particles with diameters ranging from 1 to 2 mm. The optimum sinterization temperature was found at 620 °C, at this temperature, a number of necks between Al particles surfaces were observed; indicating a good cohesion between Al particles, while keeping the porous structure of the green compact. The level of porosity was dependent of the carbamide content and the voids formed within the Al particles after the sinterization process. The sample with 60 wt.% of carbamide showed the lowest yield stress value than those for the samples with 40 and 50 wt.%. The strain values significantly increased when the carbamide content increased from 40 to 60 wt.%. Finally, the results obtained from a new sintering device for producing metallic foams at temperatures below 900 °C are also discussed.

Keywords: Aluminum foams; Cellular metals; Powder metallurgy; Sintering dissolution process

1. Introduction

In recent years, the interest in metallic foams has widen for several industrial applications, as the properties obtained as a result of the combination of their cellular structure and metallic properties are found to be rather attractive [1]. The most common application, in particular for Al-foams, includes crash impact absorbers, noise reduction systems and lightweight panels for automotive industry; heaters and heat exchangers, fluid filters, catalysis supporters among others for functional industry and some application in aerospace and biomedical industries [1-3]. This range of applications of, in particular, Al-foams is obtained for its good mechanical properties combined with low weight [4].

There are a number of processing-routes developed to produce metallic foams, however, they can be grouped mainly in the following categories: 1) according to the nature of metal (liquid and solid), 2) melt-foaming agents, 3) powder-space holders, 4) investment casting and 5) melt infiltration [5- 6]. In order to produce open-cell structures is necessary the employ of internal removable patterns or space holders [5-11]. The application of materials with

sacrificial functions in other areas, such as surface engineering has been reported, here sacrificial coatings and its effect on the Al-Al₃Ni ultrafine eutectic formation was investigated [12]. However, the present author have reported the formations of highly porous metallic foams without the use of such removable patterns or foaming agents, for alloys with specific characteristics [13].

In the powder method, called Sintering and Dissolution Process (SDP), metallic powder and a water-soluble phase are mixed and mechanically compacted to produce a double-connected structure of both phases (metal and space holder, SH). Then the compact is sintered at temperature close or above the melting point of the metallic phase to produce a net-shape structure with bonded particles. Finally, the water-soluble phase is removed by leaching the compact to produce open-cell metallic foams. The advantages of this process are that the porosity of final foam is closely fixed and can be modified by adjusting the water soluble/metallic particles volume ratio in the powder compact [1, 14]. In this process, there are a number of parameters that affect the final structure of the foam produced, which can be associated to: 1) materials (morphology, composition,

etc.), 2) compaction process (pressure and time), and 3) sinterization conditions (time, temperature and atmosphere). From the above, an adequate control of such parameters is essential in order to obtain foams with the advantages that this process offers. From this, the aim of this work is to analyze the effect of SH diameter, SH concentration and the sintering temperature on the formation of Al foams, and their respective effect on the mechanical properties. The introduction of a sintering device for producing metallic foams at temperatures below 900 °C will be also presented.

2. Experimental

The materials employed for the processing of metallic foams were gas atomized Al powder with irregular shape, particle size in the range of 75–200 μm (Figure 1a) and a purity of 99.5 %. For the space holder, spherical carbamide granulates provided by Sigma-Aldrich with 99 % of purity and particle sizes ranging from 1 to 2 mm were used (Figure 1b). To obtain the Al/carbamide green compact, these materials were mixed using a double cone mixer during 15 minutes. With the aim of ensuring good adhesion among Al powders and carbamide granulates, 2 vol.% of ethanol was sprayed onto the carbamide granulates before the mixing stage in order to obtain a sticky surface. Then, the mixture was poured into the steel mold and then, it was uniaxially compacted to produce cylindrical samples of around 13 mm in diameter and around 15 mm in length. The pressure used for the compaction stage of the Al/carbamide mixture was 300 MPa, for all samples. The carbamide content of the green compact was dissolved by immersion in a gently stirred water bath at 25 °C during two hours. It is worth mentioning that dissolution process was carried out before the sintering process.

For the sintering process, in this work we are proposing a new device that could be used for producing aluminum foams and other metals with sintering temperatures below 900 °C. With the use of this device, it is intended to get the maxima advantages that DSP provides. Figure 2 shows the home-manufactured device used for this research. This consists on the following parts: (a) stainless steel (*ss*) chamber rounded by an *ss* tube spiral, (b) a valve system for controlling the vacuum and gas injection, (c) a graphite flexible seal and (d) a heating system, which could be an electrical resistance furnace or a heating device with vertical chamber. The latter component could be part of the device or could be external.

The sample is located inside of the *ss* chamber, as shown in Figure 2. The bottom part of this chamber is attached to the top part, and sealed with the flexible

graphite seal. Once this process has been completed, the vacuum valve is opened until a pressure of 6×10^{-2} torr is reached. After this, five purges with high purity Ar are carried out. Then, a constantly controlled Ar flow is introduced through the *ss* spiral, being heated during its trajectory from the top of the device to the inlet, which is located at the bottom of the equipment. The combination of the Ar flow and the spiral setup not only minimizes the amount of oxygen inside the chamber, but also it keeps the sample at the desired temperature, and takes away all the fumes produced during the sintering process, leaving a clean and inert atmosphere surrounding the sample. Finally, the green compacts were sintered at temperatures from 600 °C to 660 °C (with increments of 20 °C in each experiment) in order to determine the optimum sinterization temperature, T_s . The process treatment at 660 °C was only taken for temperature control purposes.

The foam relative density, ρ , and its, porosity, P_p , were determined through the equations (1) and (2) [14, 15], respectively.

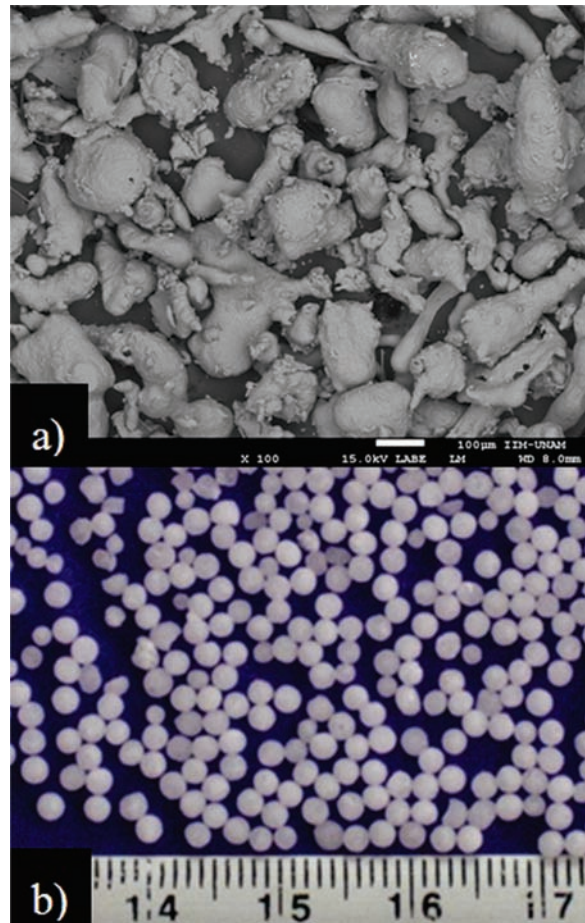


Figure 1. a) SEM micrographs of the Al powders and b) image of the carbamide

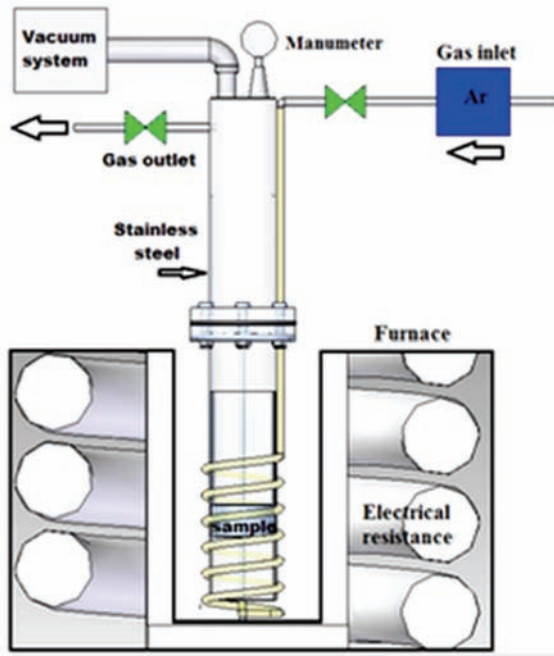


Figure 2. Proposed sintering device

$$\rho = \frac{V_{Al} \cdot \rho_{SH}}{V_{Al} \cdot \rho_{SH} + (1 - V_{Al}) \cdot \rho_{Al}} \quad (1)$$

$$P_f = (1 - (\rho_f / \rho_{Al})) \cdot 100 \quad (2)$$

Where, ρ is the theoretical relative density of the foam, ρ_{Al} is the Al density, V_{Al} is the Al volume fraction in the mixture, ρ_{SH} is the carbamide density and ρ_f is the foam density. The densities of green compact and foams were determined using the conventional equation $\rho = m/V$ (m =mass, V =volume). The pore size and distribution of the Al-foams was analyzed using stereomicroscope Olympus SZX16. Field Emission Scanning Electron microscope Jeol JSM-7600F was used to observe the neck formation between Al particles and the pores interconnection. Finally, the mechanical properties of the specimens were measured by means of standard compression tests using an Instron 1125-5500R testing machine with a crosshead speed of 0.1 mm/min.

3. Results and discussion

3.1. Analysis of the sintering temperature effect

As expected, at a sintered temperature of 660 °C the individual Al-particles melted down during the process, the structure of the foam completely collapsed, forming a solid ingot. When the sintering temperature was reduced down to 640 °C, the Al foam sample partially collapsed, as this temperature is rather close to the Al melting temperature. Here, the Al particles were mostly consolidated, forming much

larger particles or clusters and few necks between the initial Al particles were observed. This can be attributed to the sintering temperature, which softens the Al powders, given place to the formation of such clusters. It is worthy of note that the number of interparticles pores also dropped drastically (Figure 3a). The partly collapsed Al foam shown in Figure 3a corresponds to the sample with 60 wt.% of carbamide.

At 620 °C a number of necks between Al particles surfaces were observed, indicating a good cohesion between Al powders (Figure 3b). At this sintering temperature, the porous structure resembles that of the green compact. This fact can be observed in the resulting foam shown in Figure 3b. From these results, it can be suggested that 620 °C can be considered as the optimum sinterization temperature, for at least, the experimental conditions reported in this work. Finally when the sintering temperature was dropped down to 600 °C the cohesion between the Al powders was poor, as observed in Figure 3c, and the foam structure tended to crumble apart at low stresses (i.e. when handling the Al foam sample).

3.2. Analysis of the space holder concentration

Figure 4a shows the structure of the Al foam with 40 wt.% of carbamide obtained using the optimum sintering temperature (620 °C). From this figure, the foam presented a deficient open interconnection between pores and the existence of blocking walls between pores, reducing the possibility to produce an open-cell foam structure. With the increment of the carbamide concentration, up to 50 wt.% (Figure 4b), the interconnection of the foam also increases (with four pores interconnected). Finally, the foam with 60 wt.% of carbamide (Figure 4c) presented the highest increment of the interconnection, practically, with all pores interconnected. For 50 wt.% and 60 wt.% an open-cell foam structure was obtained.

In terms of the microstructure, these results indicate that the optimal concentration of carbamide (for the present size) to produce open-cell metallic foams is 60 wt.%. Green compact samples with contents of 40 and 50 wt.% of carbamide are not suggested for the production of Al-foams with good interconnected pores, under the conditions proposed in this work. At lower carbamide contents than the reported here, the pores interconnections are totally blocked, and at higher carbamide contents, the network of metallic foams collapses during the dissolution process. On the other hand, the metallic particle sizes used in the manufacturing of Al-foams promotes the formation of micropores, which increased, slightly, the foam porosity (Figure 3b). The analysis of relative density (Absolute Density: expresses the magnitude of mass and volume of a

substance and Relative Density: is the ratio between the density and density of the other reference substance is a dimensionless number) is important in order to understand the lightweight properties. The values of relative density also give an idea of the foam porosity and the interconnection type between the Al particles. Figure 5a shows the behavior of relative density as function of Al concentration for two sizes of carbamide granulates and two different sintering temperatures. As it can be observed, the relative density decreases, as does the Al concentration, ensuring the formation of foams with an open pore structure. On the other hand, the observed decrement of the relative density could be associated to the large carbamide particles size, with respect to the size of Al powder, which promotes this level of porosity. The experimental relative density values are lower than theoretical ones; this is attributed to the size and shapes of Al particles, in addition to the bonding/union between them, during that sinterization step. Figure 5b shows that the experimental values of porosity, for all compositions, are higher when compared to the theoretical one. It is though, that this behavior is due to the sum of the porosity left by the space holder and the small amount of porosity caused

by the Al spheres/particles packing (space produced between Al particles during the compaction). Although the vast majority of the porosity produced was attributed to the carbamide particles.

From the above, it can be concluded that the foams manufactured with carbamide contents of 60 %, exhibited porosity about 70 % and the high P_f value is essentially caused by two contributions: a) The

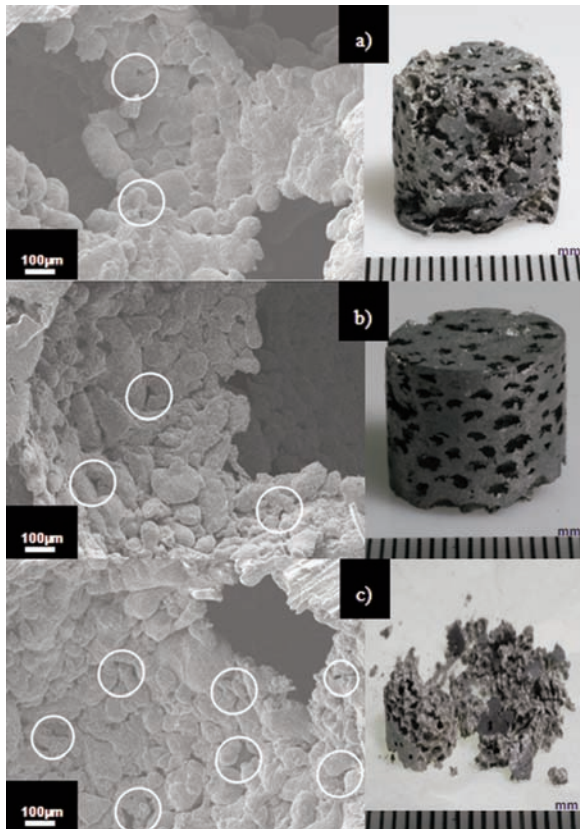


Figure 3. Al foam images a) sintered at 640°C, b) sintered at 620°C and c) sintered at 600°C

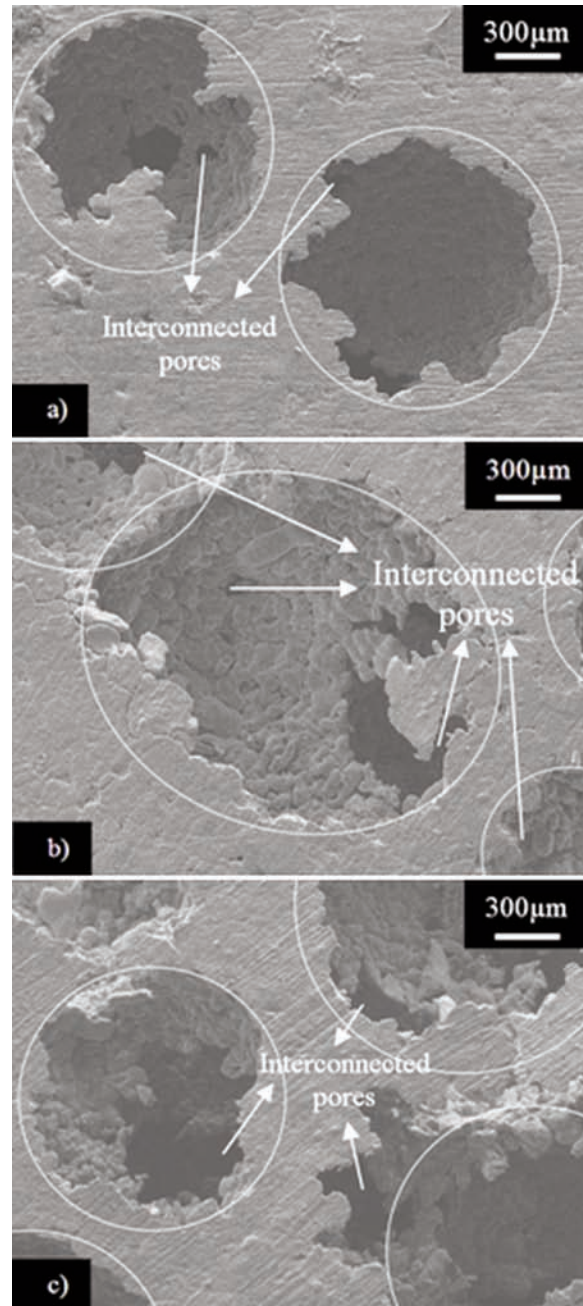


Figure 4. Scanning Electron Microscopy secondary electrons images of metallic foams series containing: a) 40 wt.%, b) 50 wt.% and c) 60 wt.% carbamide

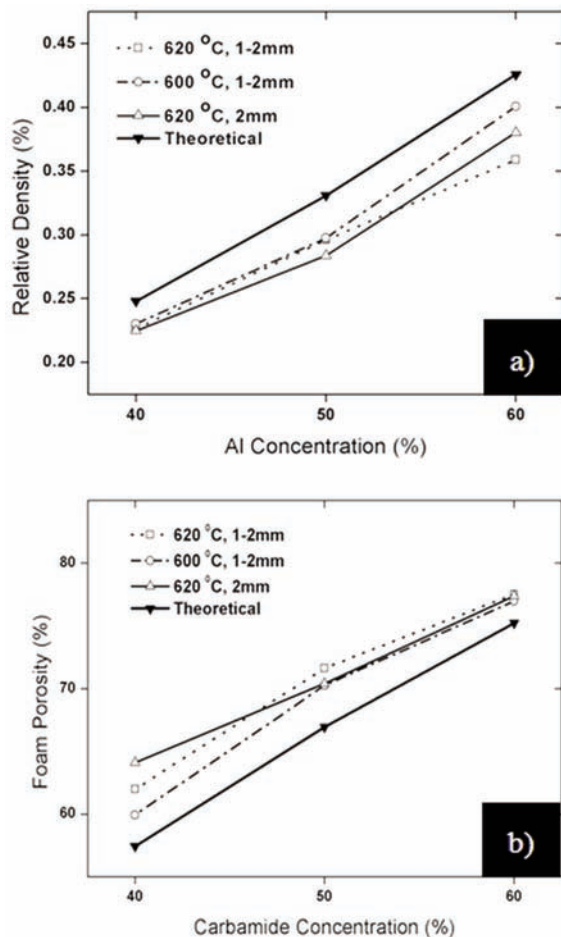


Figure 5. a) Relative density and b) porosity of Al foams after the sinterization process and cleaning, as a function of the Al concentration and carbamide content respectability

carbamide content, which generates the porosity after the dissolution, and b) The voids formed within the Al particles after the sinterization process due to the low packing efficiency of the such particles.

3.3. Mechanical behavior

Figure 6 shows the stress (σ) strain (ϵ) curves for the foams containing 40, 50 and 60 wt.% of carbamide. For the foam of 60 wt.% the typical mechanical behavior of foamy metallic materials is observed, here three zones are clearly identified: Elastic deformation (Zone I); plateau (Zone II), where the cell edges are yielding plastically in bending; and densification (Zone III), where the structure compacts and stress rises. The behavior of the σ - ϵ curves did change, depending on the carbamide content. In the case of the sample with the minimum amount of carbamide, the behavior of the σ - ϵ curve is more closely related to that of solid aluminum, since the porous concentration is

not as high as the samples with carbamide content above 50 %. From this, the blocking walls are very large and the mechanical behavior in compression of aluminum predominates. As the concentration of carbamide increases, the slope of plateau decreases as a result of the plastic deformation of such blocking walls. Besides, the instability of serrated edges observed in zone II for all foams is also attributed to the continuous or progressing collapsed of the blocking walls.

From the same Figure 6, the compression stress for densification (σ_r in Zone III) increased slightly from $\sigma_r = 22$ MPa to $\sigma_r = 24$ MPa, for the samples with 40 and 50 wt.% of carbamide, respectively. The inverse behavior is shown when the carbamide content is increased up to 60 wt.%, where it drops down to 12 MPa. It is thought that the maximum σ_r , obtained for the sample with 50 % of carbamide, could be attributed to the combination of the blocking walls size and the good sinterization between Al particles. The strain values significantly increased when the carbamide content increased from 40 to 60 wt.%. Similar behavior was also observed in Zone II, where, if the stress is kept at certain value, the strain is drastically increased as the carbamide content increases. At 60 % of carbamide, the number of blocking walls increases leading an increment in the plastic behavior of the sample, but the blocking walls are too thin and easily break up. In contrast, in the sample with 40 % of carbamide, the blocking walls are much thicker, reducing the plastic deformation. As expected, the sample with 60 wt.% of carbamide showed a lower yield stress value than those for the samples with 40 and 50 wt.% (Zone I). A plausible explanation for

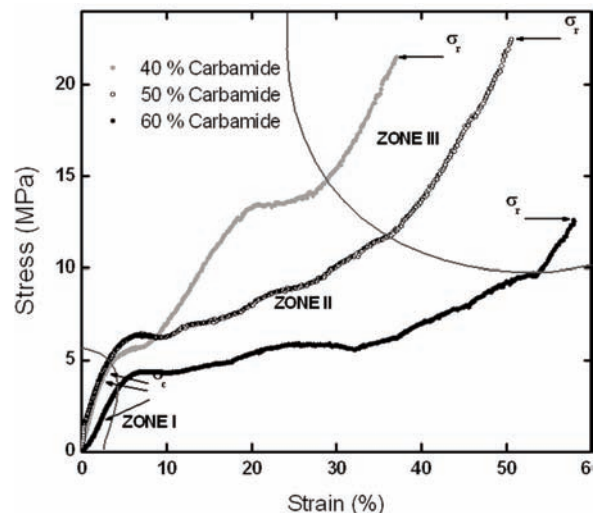


Figure 6. Stress vs strain plots for uniaxial compression tests for Al foams compacted at 300 MPa and sintered at 620 °C, containing from 40 to 60 wt.% of carbamide

this behavior could also be given in terms of the thickness of the walls formed during the sinterization, as mentioned above. However, on the other hand, the mechanical behavior could be improved with the small additions of Sn or Mg powders [17, 18].

3.4. Effect of the proposed sintering device

The proposed sintering device proved to be rather effective for sintering, in this case, Al foams. It is thought that the highly controlled atmosphere that the design/introduction of such device does allow, prevented the oxidation of the metal powder in such fashion that even at high temperatures the resulting aluminum oxide of the Al foam came from the ROW material, although further investigation is required to confirm this assumption. It is believed that the purpose of adapting the *ss* tubing spiral to the main device, i.e. introducing Ar for bottom and taking it away from the top, did help to carry all the fumes and gases produced during the sintering process out of the device, preventing the contamination of the sample that is being sintered. Therefore, by using the proposed device, the sinterization process of the Al powders could be carried out under a fully controlled atmosphere.

4. Conclusions

Metallic foams with SH concentrations between 40 and 60 wt.% of carbamide were successfully produced with the use of the proposed original device, through the powder metallurgy method known as sintering and dissolution process (SDP). The sinterization temperature of 620 °C was found to be the optimum process temperature to produce Al foams with good metallurgical bond among its constituent metallic particles. The foams manufactured with carbamide contents of 60 %, exhibited porosity ≥ 70 %. The high P_f value obtained was probably caused by the carbamide content and the voids formed within the Al particles after the sinterization process. The maximum, σ_f , values were obtained for the sample with 50 % of carbamide, this was attributed to the combination of the blocking walls size and the good sinterization between Al particles. The strain values significantly rises when the carbamide content increased from 40 to 60 wt.%. The sample with 60 wt.% of carbamide showed the lowest yield stress value of the Al foams produced. It is thought that this behavior is due to the thickness of the Al particles walls, which were produced during the sintering process. With the proposed sintering device it was possible to control, efficiently, the temperature and the atmosphere during the sintering stage.

Acknowledgements

The authors would like to acknowledge the financial support from SENER-CONACYT 151496 and SEP-CONACYT 178289 for funding the project. A. Tejada, J. J. Camacho, J. Morales-Rosales, E. Hernandez, M. Garcia de León, D. Cabrero, R. Reyes and C. Flores are also acknowledged for their technical support.

Reference

- [1] R. Surnace, L. A. C. De Filippis, A. D. Ludovico, G. Boghetich. *Mater Des.*,30 (2009) 1878-1885.
- [2] G. J. Davies, S. Zhen. *J Mater Sci.*, 18(1983) 1889-1911.
- [3] J. Banhart. *Prog Mater Sci.*, 46 (2001) 559-632.
- [4] L. J. Gibson, M. F. Ashby. *Cellular solids: Structure and Properties*. Cambridge University Press, Cambridge, UK 1997 p 2-11. 283-306.
- [5] N. Michailidis, F. Stergioudi. *Mater Des.*, 32 (2011)1559–1564.
- [6] J.O. Osorio-Hernández, M.A. Suarez, R. Goodall, G.A. Lara-Rodriguez, I. Alfonso and I.A. Figueroa. *Mater Des.*, 64 (2014) 136–141.
- [7] Y. Y. Zhao, T. Fung, L. P. Zhang, F. L. Zhang. *Scr Mater.*, 52 (2005) 295–298.
- [8] A. Irretier, J. Banhart. *ActaMater.*, 53 (2005) 4903–4917.
- [9] B. Matijasevic, J. Banhart. *Scr Mater.*, 54 (2006) 503–508.
- [10] S. Yu, J. Liu, M. Wei, Y. Luo, X. Zhu, L. Yaohui. *Mater Des.*,30 (2009) 87–90.
- [11] M. F. Ashby, A. Evans, N. A. Fleck, L. J. Gibson, J. W. Hutchinson, H. N. G. Wadley. *Metal foams: a designguide*. Butterworth–Heinemann, USA 2000 p. 6-20. 40-60.
- [12] L. Čelko, L. Klakurková, B. Smetana, K. Slámečka, M. Žaludová, D. Huid, J. Švejcar. *J. Min. Metall. Sect. B-Metall.* 50 (1) B (2014) 31 – 36.
- [13] M. A. Suarez, I. A. Figueroa, G. Gonzalez, G. A. Lara-Rodriguez, O. Novelo-Peralta, I. Alfonso, I. J. Calvo. *JAlloycompd.*, 585 (2014) 318-324.
- [14] Y. Zhao, F. Han, T. Fung. *Mater Sci Eng.*,364 A (2004) 117–125.
- [15] Y. Y. Zhao, D. X. Sun. *Scr Mater.*, 44 (2001) 105-110.
- [16] H. Bafti, A. Habibolahzadeh. *Mater Des.*, 31 (2010) 4122-4129.
- [17] A. Yan, L. Chen, H. S. Liu, F. F. Xiao, X. Q. Li. *J. Min. Metall. Sect. B-Metall.*, 51 (1) B (2015) 73-79.
- [18] I.A. Figueroa, O. Novelo-Peralta, M.A. Suárez, G.A. Lara-Rodríguez. *J. Min. Metall. Sect. B-Metall.* 49 (3) B (2013) 293 - 297